INTERFACE SCIENCE 6, 7–22 (1998)
© 1998 Kluwer Academic Publishers. Manufactured in The Netherlands.

Grain Boundary Migration in Metals: Recent Developments

GÜNTER GOTTSTEIN AND DMITRI A. MOLODOV
Institut für Metallkunde und Metallphysik, RWTH Aachen, 52056 Aachen, Germany

LASAR S. SHVINDLERMAN
Institute of Solid State Physics, Russian Academy of Sciences, Chernogolovka, Moscow distr. 142432, Russia

Abstract. Current research on grain boundary migration in metals is reviewed. For individual grain boundaries the dependence of grain boundary migration on misorientation and impurity content are addressed. Impurity drag theory, extended to include the interaction of adsorbed impurities in the boundary, reasonably accounts quantitatively for the observed concentration dependence of grain boundary mobility. For the first time an experimental study of triple junction motion is presented. The kinetics are quantitatively discussed in terms of a triple junction mobility. Their impact on the kinetics of microstructure evolution during grain growth is outlined.

Keywords: grain boundary mobility, triple junction motion, impurity drag, orientation dependence, migration mechanisms

1. Introduction

Grain boundary motion (GBM) is one of the classical unresolved problems in materials science. Despite a long history of research on GBM, there is persistent, even increasing interest in this matter. The main reason is that the GBM determines the evolution of the granular microstructure in the course of recrystallization and grain growth, i.e., the grain morphology and crystallographic texture of polycrystals which, in turn, determine their physical, chemical and mechanical properties. Grain growth studies in polycrystals provide only average grain boundary (GB) mobilities, i.e., mobilities averaged over a large number of grain boundaries. If all boundaries would behave alike, this would be a reasonable experimental conduct. As will be shown below, however, this is far from the truth. In contrast, GBM is strongly affected by GB crystallography and chemical composition besides temperature and pressure during annealing. Such dependencies cannot be obtained from experiments on polycrystals, but only from the behavior of individual grain boundaries, as will be shown below.

Fundamental results have been established from the investigation of individual boundaries, i.e., from bicrystal experiments [1–10]. Firstly, it was demonstrated that the velocity v of grain boundary migration is proportional to the driving force p per atom, $p/kT \ll 1$. This condition always holds for recrystallization and grain growth. There were also reports that $v \sim p^n$, $n > 1$, but it was shown also that the observed deviations from the linear dependence had to be attributed to the action of the side effects [11, 12]. Secondly, the investigations disclosed that the temperature dependence of the velocity of grain boundary motion follows an Arrhenius dependency. The respective activation energy of grain boundary migration is a very complicated issue that will be discussed below. An important result of bicrystal experiments is the proof of a misorientation dependence of the velocity of grain boundary motion, i.e., different grain boundaries have different kinetic properties [3] (Fig. 1). In particular, it was found that grain boundaries with special misorientations (low Σ coincidence boundaries) have extremal properties, for instance with regard to their mobility.

It is common experience that even small amounts of impurities reduce drastically the velocity of grain boundary motion. This has been interpreted theoretically by the drag effect of impurities owing to their joint motion with the boundary [13–15]. Consequently,

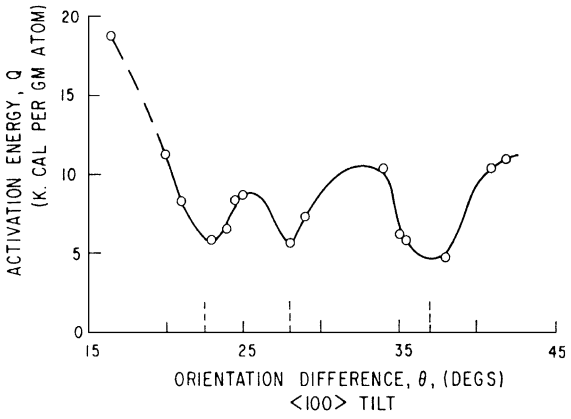

Figure 1. Measured activation energies (Q) vs. orientation difference, θ, for $\langle 100 \rangle$ tilt boundaries in zone refined lead [3].

the activation energy of grain boundary motion should correspond to the sum of the activation energy for impurity diffusion and the energy of interaction between the adsorbed atom and the boundary. This conclusion, however, is at variance with experimental results [1]. Moreover, the impurity drag theories do not take into account grain boundary structure and thus, the orientation dependence of impurity segregation, which may be drastically different for special and non-special boundaries.

In addition to dissolved impurities small particles of a second phase constitute one of the most effective drag factors in grain boundary migration. The drag by particles on a moving grain boundary is usually considered in the Zener approximation, where the particles act as a stationary pinning center for the boundaries [16]. However, it is well known that inclusions in solids are not immobile and that the particle mobility drastically increases with decreasing particle size. Therefore, small particles can move along with the boundary and severely affect grain boundary migration [17]. Since the current paper is confined to single phase material, particle effects will not be addressed, though.

At last, it is stressed that current theories of grain growth and microstructure development tacitly assume the motion of free grain boundaries, which do not interact with each other. This implies that triple junctions which are an integral part of a grain boundary network are only to preserve thermodynamical equilibrium where boundaries meet, but do not affect the kinetics of microstructure evolution. This assumption has never been verified, however.

In the following we will report on recent progress in the understanding of the migration of grain boundaries and grain boundary systems, in particular by addressing the above mentioned unresolved issues.

2. Experimental

In spite of a considerable body of research dedicated to GB migration, there are only few investigations conducted under reproducible experimental conditions. The major requirements for a proper experiment on GBM include a controlled driving force, a continuous tracking of GB displacement, an accurate and reproducible of GB crystallography and, of course, a controlled chemistry of the material.

Several boundary geometries were designed to move a boundary with a controlled or even constant driving force. A sketch of a bicrystal specimen where the GB moves under a constant driving force is given in Fig 2. The driving force p of GBM is provided by the surface tension of the curved GB: (a) $p = 2\sigma/a$ and (b) $p = \sigma/a$, where σ is the GB surface tension and a is the width of the shrinking grain. The advantage of such a geometry is that the GB remains self-similar during migration [18, 19].

There are two principally different ways to determine the velocity of a GB. In the discontinuous method the location of the boundary is determined at discrete

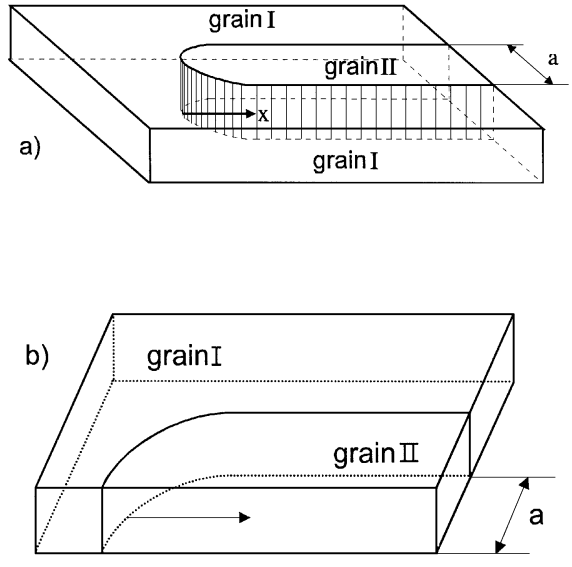

Figure 2. Geometry of used bicrystals, driving force: (a) $p = 2\sigma/a$, (b) $p = \sigma/a$.

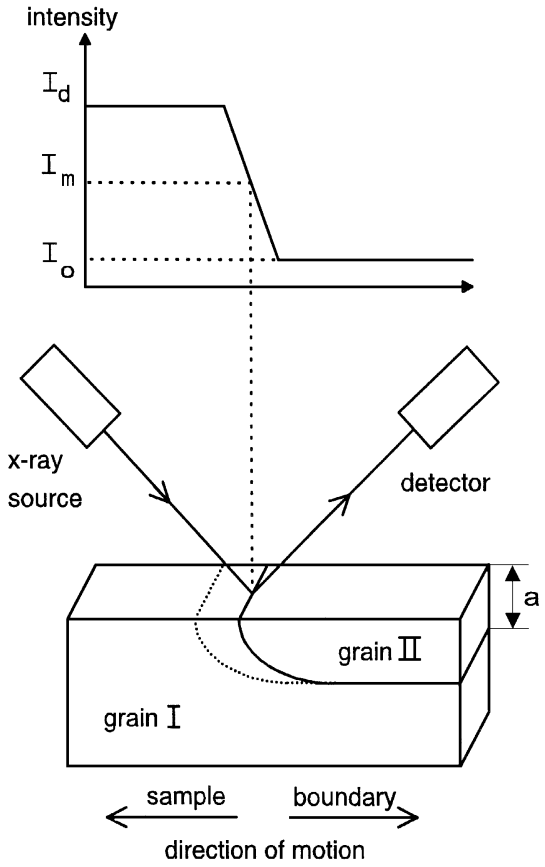

Figure 3. Bicrystal geometry for grain boundary motion measurements under a constant driving force and measurement principle of the XICTD.

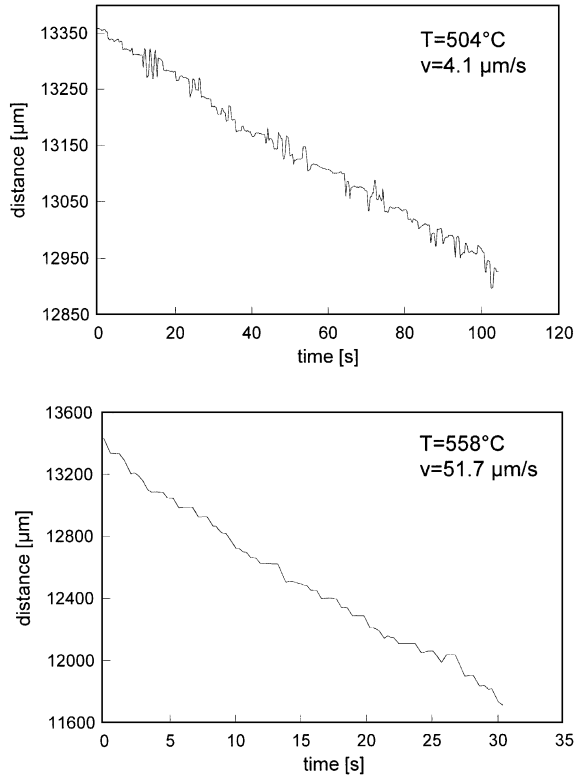

Figure 4. Distance-time diagrams for 40.5° ⟨111⟩ tilt grain boundary migration at two different temperatures.

time intervals by the position of a GB groove. The advantage of this method is its simplicity, but its main shortcoming is that the measured GB velocity is averaged over the large interval of time between consecutive observations. In contrast, the continuous method requires to determine the boundary position at any moment of time without forcing the GB to stop. This is achieved by utilizing the discontinuity of crystal orientation at the GB.

There are various techniques to distinguish different crystal orientations, e.g., the reflection or transmission of polarized light [20, 21], photoemission [22], X-ray topography [23] or X-ray diffraction [24, 25]. The principle idea of the X-ray Interface Continuous Tracking Device (XICTD) can be understood from Fig. 3. The bicrystal is placed in a goniometer in such a way that one grain is in Bragg position while the other is not. If the X-ray spot is located on the GB, the intensity of the reflected beam should be intermediate in value between the I_0 and I_d (Fig. 3). When the boundary moves the sample must be accordingly displaced so that the reflected X-ray intensity remains constant during the GBM. Thus, the velocity of the moving GB is equal to the speed of sample movement at any moment during the experiment. Due to the constant driving force the boundary is expected to be displaced with a constant rate. This is indeed observed (Fig. 4). The device can measure a GB velocity in a wide range between 1 μm/s to 1000 μm/s and allows up to 4 measurements of the boundary position per second. Its inaccuracy depends on the frequency of measurement and amounts to less than 2% [25]. The hot stage of the device allows a sample temperature between 20°C and 1300°C. During the measurement of GBM the temperature is kept constant within $\pm 3^\circ$. To account for thermal expansion of the sample the Bragg angle is continuously adjusted during temperature changes. To avoid surface oxidation the sample and the hot stage are exposed to a nitrogen gas atmosphere.

During the experiment the boundary displacement is recorded. Its derivative with regard to time is the velocity v of grain boundary motion, which is related to

Table 1. Materials notation and purity.

Material	Al I	Al II	Al III	Al IV	Al V
Total impurity content, ppm	0.4	1.0	3.6	4.9	7.7

the driving force p by the boundary mobility $m = v/p$. For convenience we use the reduced boundary mobility

$$A \equiv v \cdot a = A_0 \exp\left(-\frac{H}{kT}\right) = m\sigma, \qquad (1)$$

where H is the activation enthalpy of migration and A_0 the pre-exponential mobility factor. In the following we refer to it as mobility for brevity.

Apparently, this method avoids any interference of the measurement with the process of GBM, and, is sufficiently versatile to be applicable to a great variety of materials. The current bicrystal studies were conducted on Al of different purity, as given in Table 1.

In order to study the triple junction motion, not only the displacement should be measured, but also the angles at the triple junction. A special device was designed which makes it possible to observe and record the motion of a GB system in polarized light. The experiments were carried out in the temperature range 300–410°C. For each temperature the velocity of the triple junction and the vertex angles 2θ were determined. Tricrystals of Zn (99.999 at%) with a triple junction were grown by a directional crystallization technique [26].

3. Misorientation Dependence of Grain Boundary Mobility

3.1. Tilt Boundaries

From recrystallization and grain growth experiments it is evident that small angle boundaries move much more slowly than large angle boundaries. But even for large angle grain boundaries the mobility depends on axis $\langle hkl \rangle$ and angle φ of misorientation, as was already shown in the past, for instance by Aust and Rutter [3] or Shvindlerman et al. [8–10, 28] for tilt grain boundaries. Studies of the mobility of tilt grain boundaries in Al bicrystals [9] have shown that the mobility of low Σ coincidence boundaries (special boundaries) exceeds the mobility of random (non-special) boundaries. Among all tilt boundaries those with $\langle 111 \rangle$ rotation axis and rotation angle of about 40° were found to have the highest mobility, which is associated with the special $\Sigma 7$ (38.2°$\langle 111 \rangle$) tilt boundary.

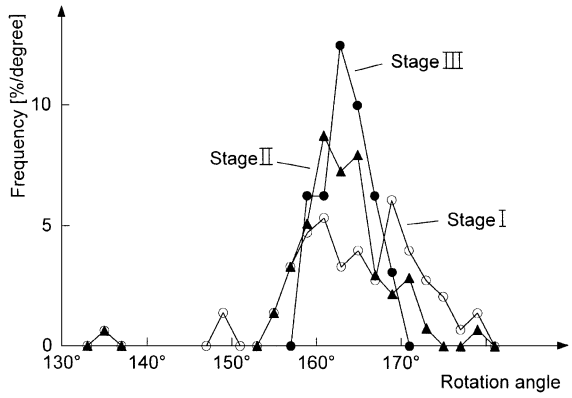

Figure 5. Growth selection in 20% rolled aluminum single crystals as observed at three consecutive stages. Frequency of the rotation angles around the best fitting $\langle 111 \rangle$ rotation axes [29].

However, from growth selection experiments [29, 30] it was known that the rotation angle of the fastest boundary was invariably larger than 38.2° even consistently larger than 40° (Fig. 5).

Owing to the importance of maximum growth rate boundaries for texture formation during recrystallization and grain growth we addressed this obvious discrepancy, and we investigated the misorientation dependence of grain boundary mobility on a fine scale in the angular interval $37° - 43° \langle 111 \rangle$ with angular spacing $0.3° - 0.6°$ [31, 32]. The experiments revealed that both the activation enthalpy and the preexponential factor were at maximum for a misorientation angle $\varphi = 40.5°$ and at minimum for the exact $\Sigma 7$ orientation (Fig. 6). Therefore, one is tempted to conclude that the $\Sigma 7$ boundary has the highest mobility. However, the mobility of boundaries with different misorientation angles do have a different temperature dependence, and there is a temperature, the so-called compensation temperature T_c, where the mobilities of all investigated boundaries of differently misoriented grains are the same. As a result, for $T > T_c$, the mobility is higher for grain boundaries with higher activation energy, in particular it is at maximum for $\varphi = 40.5°$, while for $T < T_c$ the exact $\Sigma 7$ boundary moves fastest (Fig. 7).

This result explains the apparent contradiction between growth selection experiments and recrystallization experiments. The problem resulted only from the wrong tacit assumption that the preexponential factor is

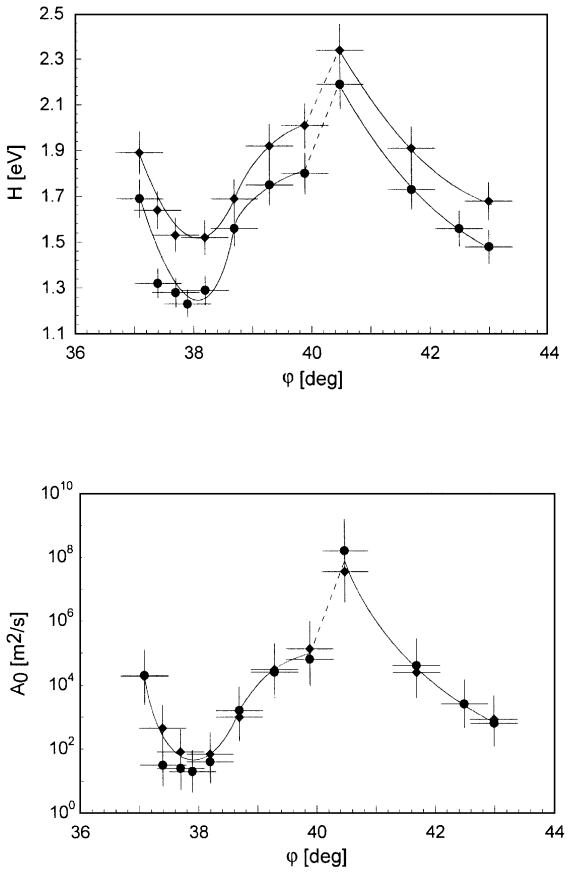

Figure 6. Activation enthalpy H and preexponential factor A_0 for ⟨111⟩ tilt boundaries in pure Al of different origin (●—Al I; ♦—Al II).

essentially independent of misorientation so that only the activation enthalpy controls mobility. Growth selection experiments have to be conducted at very high temperatures (above 600°C), i.e., in the temperature regime, where, according to results of the current study, the mobility of the 40.5° ⟨111⟩ boundary is the highest due to its high preexponential factor. The reason for the changing maximum mobility orientation in different temperature regimes is obviously the orientation dependence of both, the activation enthalpy and the preexponential factor. In fact, both are related to each other in a linear fashion (Fig. 8), i.e.,

$$H = \alpha \ln A_0 + \beta \tag{2}$$

where α and β are constants. This correlation is referred to as the compensation effect and will be discussed in Section 6.

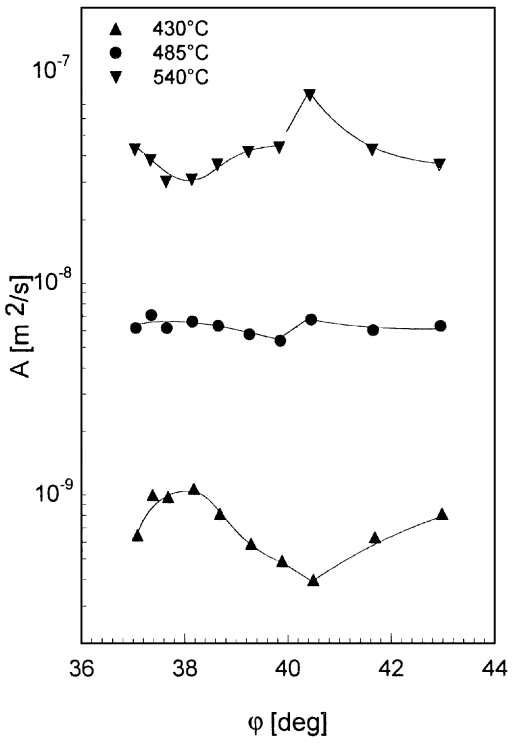

Figure 7. Mobility dependence of ⟨111⟩ tilt grain boundaries on rotation angle in pure Al at different temperatures.

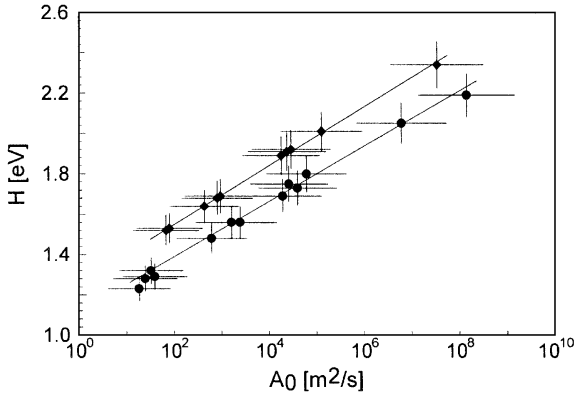

Figure 8. Dependence of migration activation enthalpy on preexponential mobility factor for ⟨111⟩ tilt grain boundaries in Al I (●) and Al II (♦).

3.2. *Dependence on Grain Boundary Plane*

Grain boundary mobility is known to depend not only on misorientation, but also on the orientation of the grain boundary plane. This is particularly evident for coherent twin boundaries, which are much less mobile than incoherent twin boundaries despite of identical

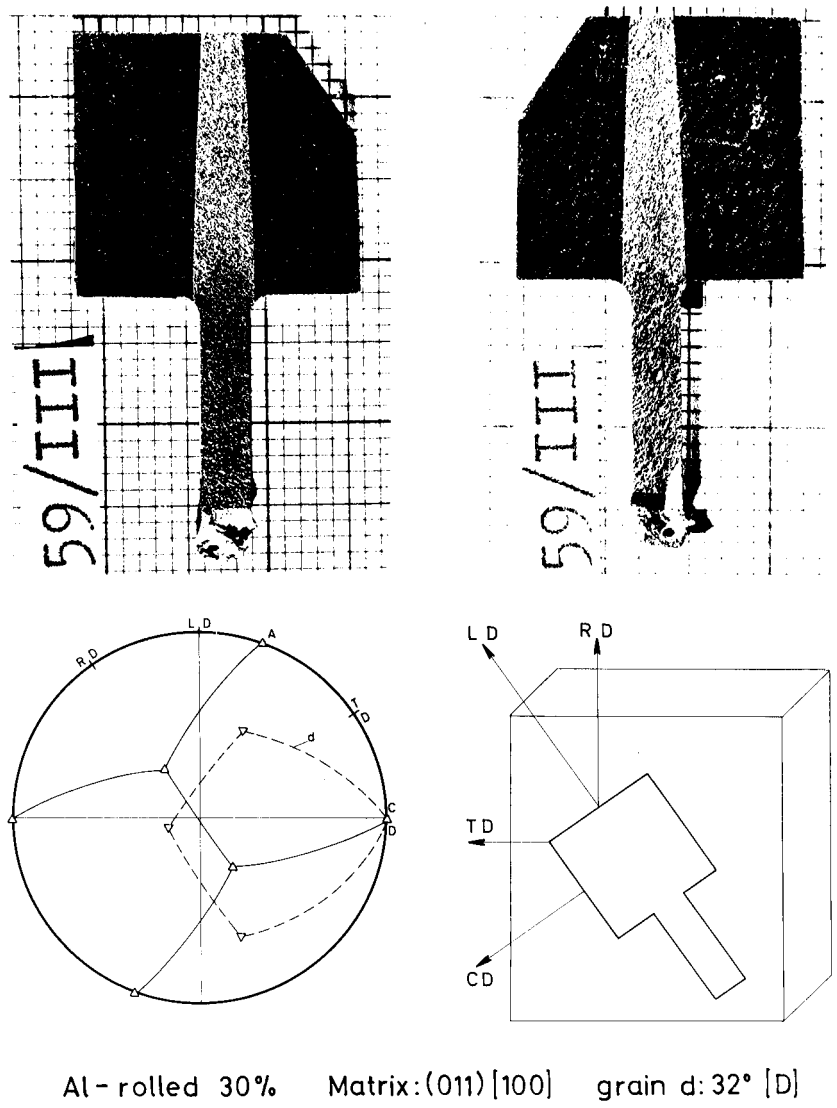

Figure 9. Anisotropic growth of a grain in rolled Al. Prior to annealing the grain boundary was located at the top of the handle. Micrograph shows front and back face of the specimen. The long straight grain boundaries are approximately perpendicular to the ⟨111⟩ rotation axis (twist boundaries).

misorientation across the boundary. But anisotropy of grain boundary mobility can also be observed for misorientations other than twin relationships, in particular grain boundaries of a misorientation with ⟨111⟩ rotation axis. For such orientation relationships tilt boundaries can move orders of magnitude faster than pure twist boundaries (Fig. 9) [33]. By definition, it is impossible to study the effect of grain boundary orientation on its mobility by utilizing grain boundary curvature as a driving force. Such experiments—as used in this study—provide only an average mobility of all involved boundary orientations. All pure tilt boundaries of the same misorientation exhibit essentially the same mobility as evident from the preservation of shape of a curved tilt boundary during migration. On the other hand, planar boundaries are difficult to move under a constant and controlled driving force, except when utilizing anisotropic volume properties, like elastic constants or magnetic susceptibility. However, such experiments are needed to study the anisotropy of grain boundary mobility, i.e., the effect of the twist component of a boundary on mobility. Such studies are currently in progress by utilizing high magnetic field facilities.

4. Effect of Impurities on Grain Boundary Mobility

4.1. Impurity Drag

The strong interaction of impurities and grain boundary structure is particularly obvious in ⟨100⟩ tilt boundaries in Al (Fig. 10) [8]. For ultrapure and very impure material the mobility of ⟨100⟩ tilt boundaries was found to be independent of rotation angle, irrespective whether special or non-special boundary. For intermediate (although high) purity material, the mobility strongly depends on rotation angle, distinguishing special and non-special boundaries. Such behavior was never reported for tilt boundaries in Al with axis other than ⟨100⟩.

The effect of impurities on grain boundary motion was addressed by the impurity drag theories of Lücke and coworkers [13, 15] and Cahn [14]. These theoretical approaches are based on the assumption that there is an interaction between impurities and the grain boundary such that the impurities prefer to stay with the grain boundary and, therefore, during grain boundary migration move along with the boundary. Accordingly, the boundary becomes loaded with impurities and will move more slowly than the free (unloaded) boundary. This manifests itself in a high activation energy and a concentration dependent preexponential factor for the loaded boundary. The theories predict that the activation energy is independent of impurity concentration and that the preexponential factor decreases with increasing impurity content in a hyperbolic fashion. This is at variance, however, with experimental results. As obvious from Fig. 11 the activation energy

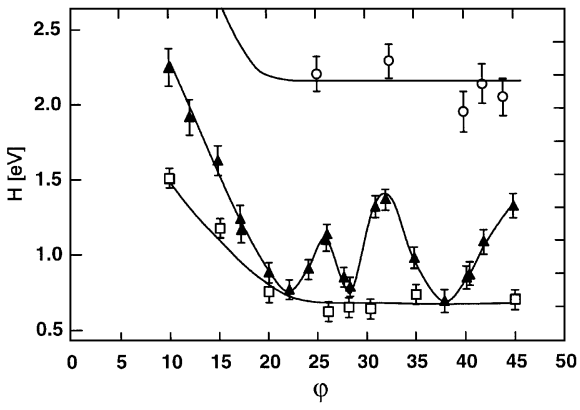

Figure 10. Dependence of the activation enthalpy of migration for ⟨100⟩ tilt grain boundaries in Al of different purity: □—99.99995 at%; ▲—99.9992 at%; ○—99.98 at%.

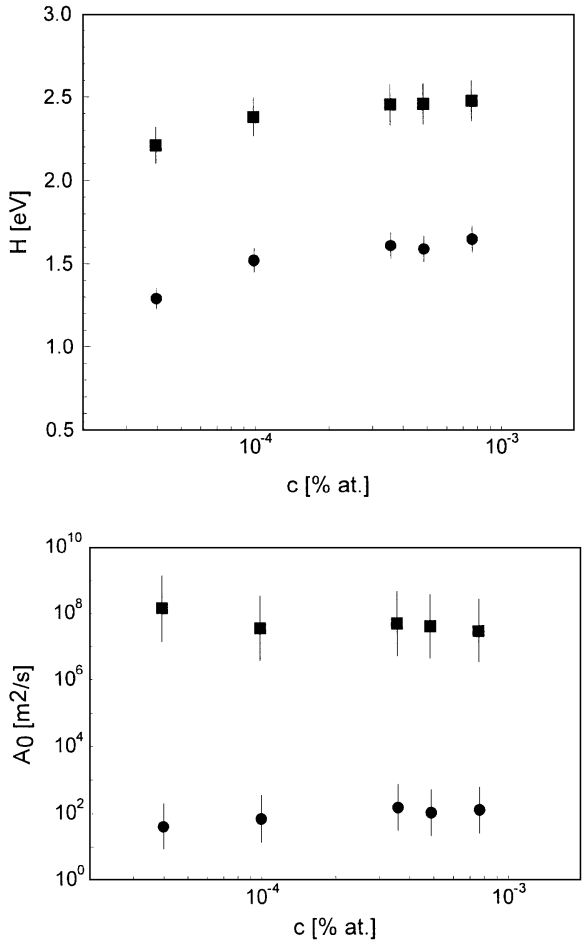

Figure 11. Dependence of activation enthalpy H and preexponential factor A_0 on impurity concentration in pure Al for 38.2° (●) and 40.5° (■) ⟨111⟩-tilt grain boundaries.

changes with concentration actually more strongly than the preexponential mobility factor does. This experimental result can only be understood in the conceptual framework of the impurity drag theory, if an interaction among the impurities in the grain boundary is taken into account, i.e., by treating the chemistry in the boundary as a real solution rather than an ideal solution. Assuming thermal equilibrium in the bulk and in the boundary, the chemical potential μ_i of the alloy constituents (impurities) must be equal throughout. For a binary alloy with concentrations c_1 and c_2

$$\mu_1^b\left(\sigma, T, c_1^b\right) = \mu_1^v(p, T, c_1) \tag{3a}$$

$$\mu_2^b\left(\sigma, T, c_2^b\right) = \mu_2^v(p, T, c_2), \tag{3b}$$

where the index b refers to the grain boundary, and the index v denotes bulk properties, σ is the grain boundary

surface tension. The activities a_i of the impurities in bulk and boundary are related by

$$\frac{a_1^b}{a_1} = \left(\frac{a_2^b}{a_2}\right)^{\frac{\omega_1}{\omega_2}} \cdot \mathrm{e}^{\frac{\omega_1(\sigma_2-\sigma_1)}{kT}}, \tag{4}$$

where $\sigma_i (i = 1, 2)$ are the grain boundary surface tensions of the pure constituents and $\omega_k = -(\frac{\partial \mu_k^b}{\partial \sigma})|_{p,T,\sigma_k}$ is the partial area of component k in the boundary.

For a regular solution the activities read

$$\begin{aligned} a_1 &= c_1 \exp\left(\frac{z\varepsilon \cdot (c_2)^2}{kT}\right); \\ a_2 &= c_2 \exp\left(\frac{z\varepsilon \cdot (c_1)^2}{kT}\right), \end{aligned} \tag{5}$$

where z is the coordination number and $\varepsilon = \varepsilon_{12} - 1/2(\varepsilon_{11} + \varepsilon_{22})$ is the heat of mixing. For an ideal solution in the bulk and a regular solution in the boundary, i.e., $\varepsilon = 0$, $\varepsilon^b \neq 0$, $\omega_1 \neq \omega_2$ and $c = c_1$, $B = B_0 \exp^{H_i/kT}$, H_i—interaction enthalpy of impurity atoms with the boundary

$$\begin{aligned} c_1^b = c_1 \exp\left(-\frac{z^b\varepsilon^b \cdot \left(c_2^b\right)^2}{kT}\right) \exp\left[\frac{\omega_1(\sigma_2-\sigma_1)}{kT}\right] \\ \cdot \left\{\frac{c_2^b}{c_2} \exp\left[\frac{z^b\varepsilon^b \cdot \left(c_1^b\right)^2}{kT}\right]\right\}^{\frac{\omega_1}{\omega_2}} \end{aligned} \tag{6}$$

and the boundary mobility m_b (with $c = c_1 = 1 - c_2$)

$$\begin{aligned} m_b &= \frac{m_{\mathrm{im}}}{c^b - c} \cong \frac{m_{\mathrm{im}}}{c^b} \\ &= \frac{m_0}{B_0 c} \cdot \frac{\exp\left[-\frac{H^* + H_i + (\beta-1)z\varepsilon(1-c^b)^2}{kT}\right]}{\left(\frac{1-c^b}{1-c}\right)^\beta} \end{aligned} \tag{7}$$

H^* is the activation energy for volume diffusion of the impurity atoms, m_{im}—mobility of the impurities, $\beta = \omega_1/\omega_2$.

Figure 12 reveals that under the assumption of reasonable values for the adjustable parameters in Eq. (7)

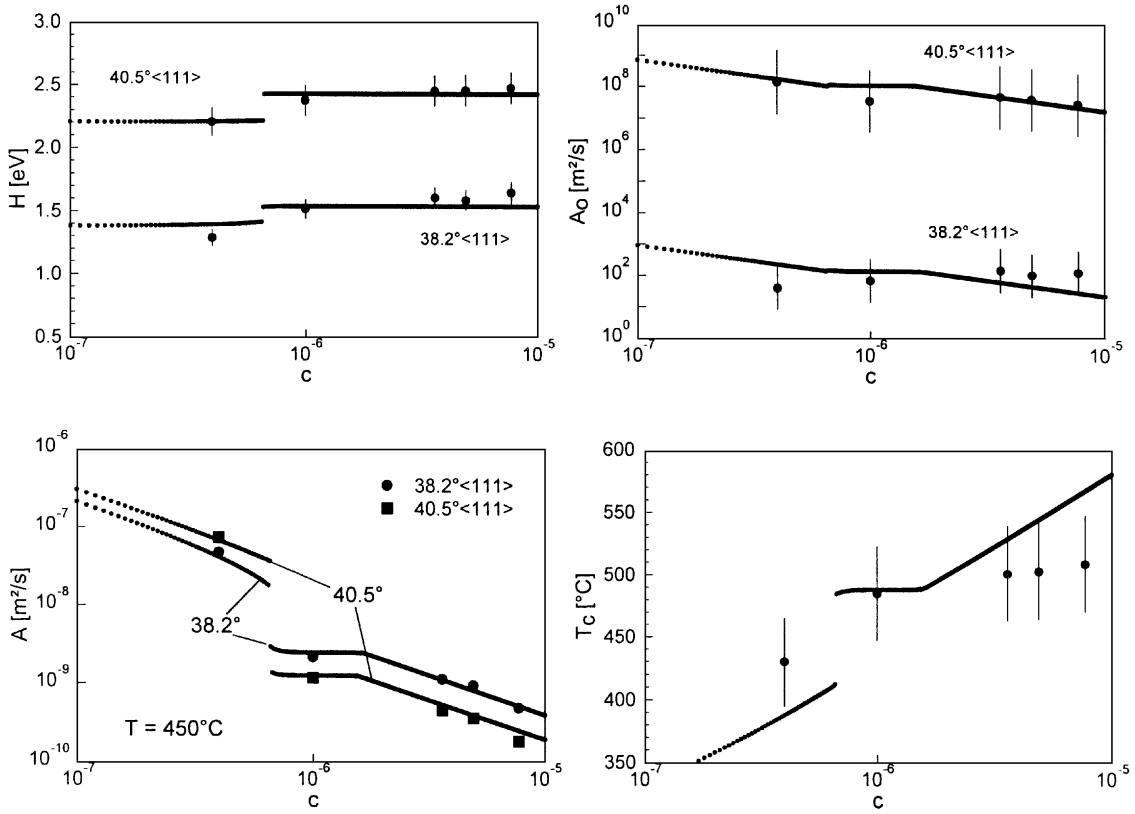

Figure 12. Experimental data (symbols) and results of calculations (lines) for two grain boundaries. Dependence of activation enthalpy H, preexponential factor A_0, boundary mobility A and compensation temperature T_c on the bulk impurity content. Fit parameters for 38.2° ⟨111⟩ boundary: $H^* = 0.68$ eV, $H_i = 0.86$ eV, $(z\varepsilon) = 0.17$ eV, $(m_0\sigma) = 3 \cdot 10^{-4}$ m^2/sec, and for 40.5° ⟨111⟩: $H^* = 1.57$ eV, $H_i = 0.86$ eV, $(z\varepsilon) = 0.24$ eV, $(m_0\sigma) = 350$ m^2/sec.

the theoretical predictions compare well to the experimental data. The observed very different behaviour of special and non-special boundaries reflects an influence of grain boundary structure on the grain boundary migration mechanism. In particular, impurities may not only have an effect on migration by impurity drag, but also by changing grain boundary structure itself. This was shown recently by Udler and Seidman in a Monte Carlo simulation study [34].

The experimental results reveal that the migration activation enthalpy is strongly affected by both, the boundary crystallography and material purity. However, in the former case the preexponential factor A_0 rises with increasing H by several orders of magnitude, while in the latter case A_0 remains at the same level. Therefore, the preexponential factor A_0 in the investigated impurity concentration interval was found to be much less sensitive to the material purity than to a change of the misorientation angle. This result allows to conclude that the observed orientation dependence of mobility (Fig. 7), determined by both H and A_0, does not only reflect the different segregation behavior of coincidence and random boundaries, as frequently proposed [3], rather it provides evidence for an intrinsic dependence of grain boundary mobility on grain boundary structure.

4.2. Mobility Enhancement by Impurities

All known experiments on bicrystals and polycrystals confirm that solute atoms reduce the rate of boundary motion. However, it is important to realize, that solute atoms not always hinder grain boundary motion, as evident from the addition of minor amounts of gallium to aluminum (Fig. 13). Our experiments were carried out on bicrystals of both pure Al (Al III) and the same Al doped with 10 ppm Ga [35]. Irrespective of the type of boundary, whether special or nonspecial, 10 ppm gallium in aluminum substantially increases grain boundary mobility, which means that it substantially speeds up recrystallization kinetics. Addition of 10 ppm Ga effectively increases the mobility of both investigated 38.2° and 40.5°⟨111⟩ tilt boundaries, but modifies the activation parameters differently. For the 38.2° ($\Sigma 7$) boundary H and A_0 increase, while they decrease for the 40.5° boundary. The orientation dependence of grain boundary mobility is strongly reduced but not entirely removed. We propose to interpret these results as a change of mechanism of grain boundary migration owing to a change of boundary structure, such that a prewetting phase transition occurs and a thin layer of a Ga-rich phase forms in the boundary.

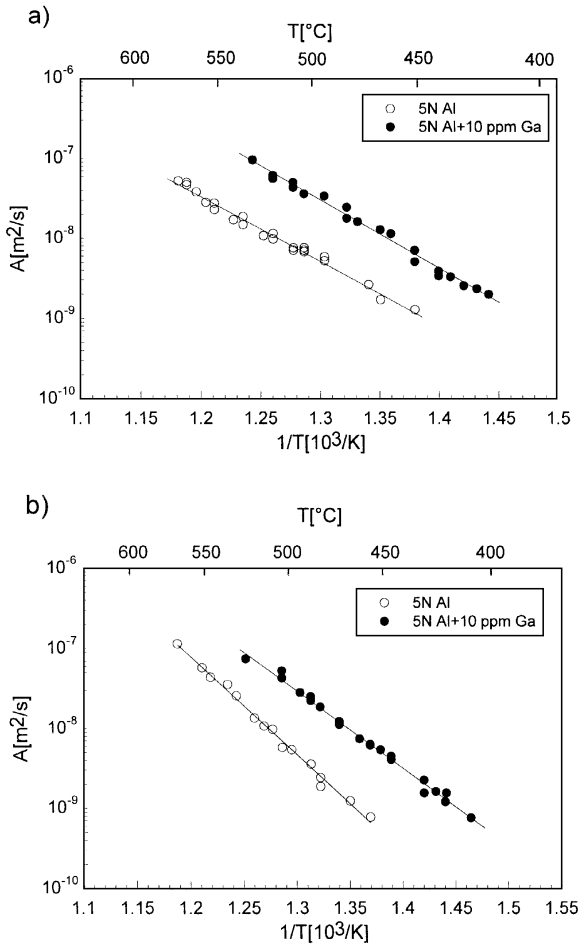

Figure 13. Arrhenius plot of mobility of (a) 38.2° and (b) 40.5° ⟨111⟩ tilt grain boundaries in pure Al and pure Al doped with 10 ppm Ga.

5. Activation Volume and Mechanisms of Grain Boundary Motion

Grain boundary motion consists of the transfer of lattice sites across the grain boundary, which results in the physical displacement of the grain boundary with regard to an external reference frame. (This definition is to differentiate grain boundary motion due to diffusion of atoms across the grain boundary without transfer of lattice sites, which would result in the displacement of the grain boundary with respect to the faces of the sample, but not with regard to the laboratory reference frame.) Generally, it is tacitly assumed that the transfer of sites across the boundary is accomplished

by the jump of individual atoms through the boundary, possibly complicated by intermediate states [36, 37]. The displacement of grain boundaries by the motion of secondary grain boundary dislocations (SGBDs) is also feasible and has been indeed ovserved [38, 39], but the thin film bicrystal experiments by Babcock and Balluffi [38] have clearly proved that SGBD motion does not constitute the intrinsic mechanism of grain boundary migration. In the literature, there have been proposals [40] and speculations [37] of more complicated migration mechanisms involving more than a single lattice site, i.e., cooperative motion of atoms (island model etc.). In fact, Jhan and Bristowe [41] and Schoenfelder et al. [42] found indications in molecular dynamics computer simulation studies of grain boundary migration that coordinated rearrangement of atoms may occur during grain boundary migration. Ahoron and Brokman [43] came to the same conclusion. However, no solid experimental proof of cooperative atomic motion as the elementary act of grain boundary migration has been presented so far. Also, the activation enthalpy of grain boundary migration does not provide unambiguous information on the mechanism of grain boundary motion, since a variety of factors, in particular specific electronic components, which are difficult to associate with a particular mechanism without understanding their very nature, contribute to its magnitude.

A thermodynamic quantity that is more directly related to the mechanism of motion is the volume change associated with the activated state of the process, i.e., the activation volume. By definition, the activation volume is the volume difference between the activated state and the ground state. This activation volume can be determined experimentally by measurement of the pressure dependence of grain boundary mobility. According to Eq. (1)

$$A = A_0 \exp\left(-\frac{H}{kT}\right) = A_0 \exp\left(-\frac{E + pV^*}{kT}\right) \qquad (8)$$

where E is the activation energy and V^* the activation volume. Accordingly

$$V^* = -kT \left.\frac{\partial \ln A}{\partial p}\right|_T \qquad (9)$$

If V^* does not change with pressure, V^*/kT equals the slope of a straight line in a plot $\ln A$ vs. p (Fig. 14) [44]. For a 32° rotation about ⟨100⟩, ⟨111⟩ and ⟨110⟩

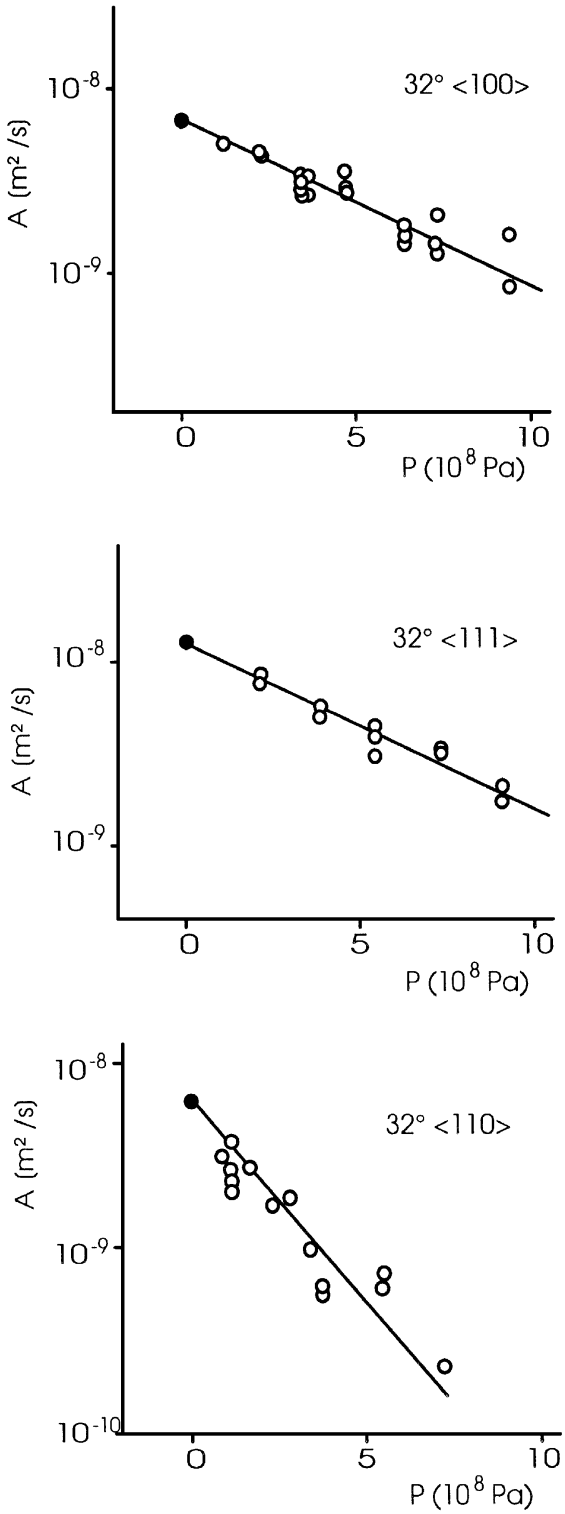

Figure 14. Pressure dependence of grain boundary mobility for tilt grain boundaries with different rotation axes but same angle of misorientation.

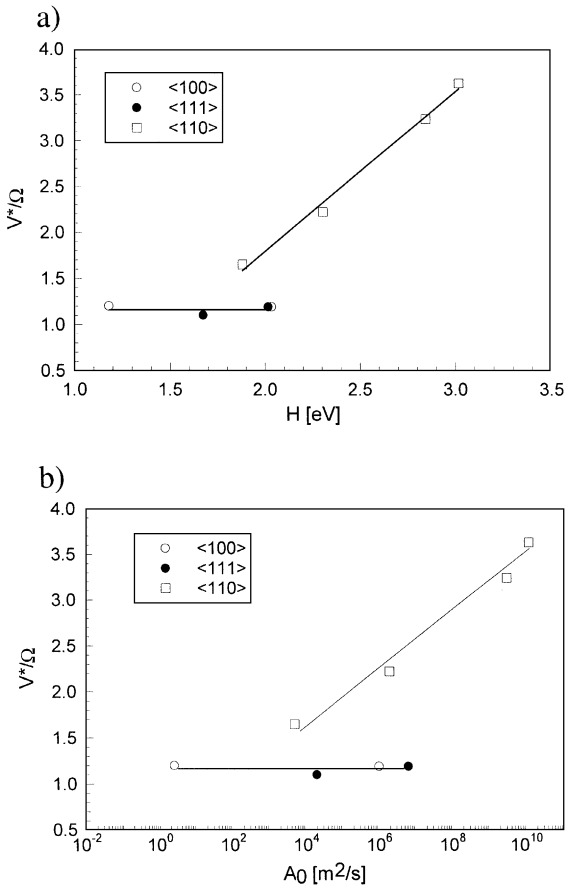

Figure 15. Activation volume V^* normalized with the atomic volume Ω as a function of the activation enthalpy H (a) and preexponential factor A_0 (b) of tilt grain boundaries with different rotation axes in Al.

it is apparent that the activation volume for the ⟨100⟩ and ⟨111⟩ boundaries is very similar but different from ⟨110⟩ tilt boundaries. The summary of all measurements (Fig. 15) revealed that the activation volume for the ⟨100⟩ and ⟨111⟩ tilt boundaries was virtually the same for all measured boundaries, including special and non-special boundaries, with a magnitude of about 1.2 atomic volumes. In contrast, the ⟨110⟩ tilt boundaries yielded a higher activation volume and showed a distinct increase of V^* with increasing activation enthalpy H. Actually V^* increased up to almost four atomic volumes for ⟨110⟩ tilt boundaries. From this result we have to conclude that at least for ⟨110⟩ tilt boundaries more than a single atom is involved in the activation process of grain boundary migration, i.e., motion proceeds by cooperative motion of atoms (group mechanism). For ⟨100⟩ and ⟨111⟩ tilt boundaries the activation volume is comparable to the activation volume for bulk self diffusion. In this case the experimental results of grain boundary motion would also justify the assumption of a monoatomic jump process. However, a cooperative motion cannot be ruled out even in this case, since the actual activation volume for a site exchange in the boundary depends on the specific site and is not well known, but maybe much less than a single atomic volume. Owing to the relationship between activation enthalpy and (log) preexponential factor (Eq. (2)), the activation volume depends in a similar way on log A_0 as it does on H (Fig. 18).

6. Compensation Effect in Grain Boundary Migration

Consistently throughout all reported measurements the activation enthalpy of grain boundary motion was found to be linearly related to the logarithm of the preexponential mobility factor (Eq. (2), Fig. 8). This so-called compensation effect was repeatedly observed in various thermally activated processes, but most distinctly in processes related to interfaces and grain boundaries. In Fig. 8 the compensation effect for ⟨111⟩ tilt GB migration in the vicinity of the special misorientation $\Sigma 7$ is shown [37]. The consequence of the specific linear dependence between the activation energy and the logarithm of the pre-exponential factor in the mobility equation is the existence of the so-called compensation temperature T_c, at which the mobilities are equal and the kinetic lines in Arrhenius co-ordinates intersect at one point (Fig. 7). The compensation temperature is not a material constant, however, but can depend on misorientation axis and composition (Fig. 16).

The observed coupling of entropy and enthalpy of activation requests that the activated state is not a random energy fluctuation in space and time, but a definite and thus reproducible although unstable state, which is described by its respective thermodynamic functions. Its attainment from the stable ground state can be associated with a first order phase transformation. In an interface we can associate the activated state with a local change of the interface structure, or more precisely, of a structure that the interface could attain if not a more stable state would exist for the given thermodynamic conditions. In this concept the compensation temperature is the equilibrium temperature for such a virtual phase transformation.

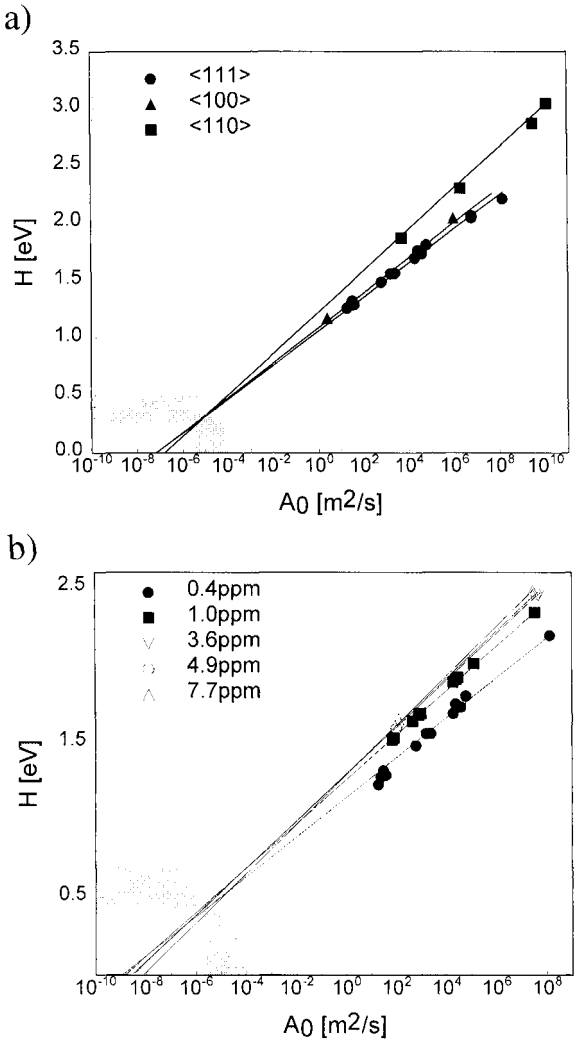

Figure 16. Compensation lines for tilt grain boundaries with different rotation axis (a) and different impurity content (b) in pure Al. (Shaded region indicates range predicted by simple rate theory.)

The compensation relation (Eq. (2)) can be easily derived under these conditions [45, 46]. As an example we consider the GB mobility m, which is known to depend on GB structure and chemistry. Let the parameter λ denote some intensive structural or chemical specification, like angle of misorientation, composition, surface tension etc. Application of the Arrhenius relation to the GB mobility m yields

$$\ln m = \ln m_0 - H_m/kT = \frac{S_m}{k} - \frac{H_m}{kT} \qquad (10)$$

where $S_m = k\ln m_0$ and H_m represent the activation entropy and enthalpy of GB mobility.

If λ changes slightly from the reference state λ_0, then S_m and H_m change accordingly

$$\ln m_0(\lambda) = S_m(\lambda)/k = \frac{1}{k}(S_m(\lambda_0) + dS_m/d\lambda|_{\lambda=\lambda_0}\cdot(\lambda-\lambda_0) + \cdots) \qquad (10a)$$

$$H_m(\lambda) = H_m(\lambda_o) + dH_m/d\lambda|_{\lambda=\lambda_0}(\lambda-\lambda_0) + \cdots \qquad (10b)$$

As S_m and H_m change only slightly, since $G_m = H_m - T\cdot S_m$ is at minimum, a linear approximation is sufficient and by solving Eqs. (10a, b) for $\lambda - \lambda_0$ yields

$$\ln m_0(\lambda) = \frac{S_m(\lambda_0) - H_m(\lambda_0)/T_c}{k} + \frac{H_m(\lambda_c)}{kT_c} \qquad (11a)$$

where

$$T_c = \frac{dH_m/d\lambda|_{\lambda=\lambda_0}}{dS_m/d\lambda|_{\lambda=\lambda_0}} = \left.\frac{dH_m}{dS_m}\right|_{\lambda=\lambda_0} \qquad (11b)$$

is the compensation temperature, i.e., the equilibrium temperature between the ground state and activated state, or equilibrium phase and "barrier" phase. This result implies that the barrier phase, i.e., the activated state, is a metastable phase closely related to the equilibrium state. It corresponds to a configuration of atoms with the smallest increase of potential energy with respect to the ground state. It seems obvious that equilibrium states occurring in the vicinity of the compensation temperature most easily satisfy this requirement. These conclusions are supported by the observation that the compensation temperature is often close to the equilibrium temperature of a nearby phase transition [46]. Of course, when considering GB phenomena, potential metastable phases need not to be confined to bulk phases.

It was shown also [46] that the compensation effect is consistent with the principles of non-equilibrium thermodynamics, in particular with the principle of the maximal rate of the system free energy reduction.

7. Motion of Grain Boundary Systems with Triple Junctions

Triple junctions along with grain boundaries are the main microstructural elements of polycrystals. Contrary to grain boundaries, the motion of which has been

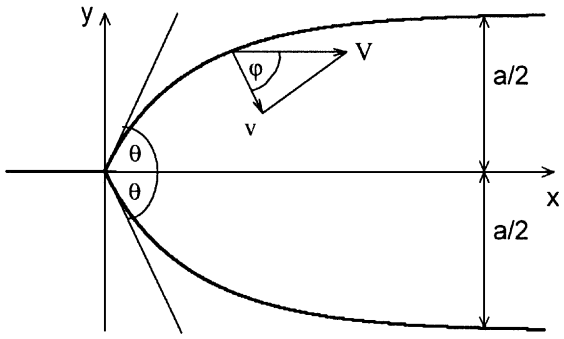

Figure 17. Grain boundary shape in a system with triple junction during steady-state motion.

frequently studied, the influence of triple junctions on GB migration was not treated at all experimentally and hardly investigated theoretically.

It is usually assumed in all studies of GB migration and grain growth that triple junctions do not drag boundary migration and that their role is reduced to preserving the equilibrium angles where boundaries meet. However, the movement of triple junctions, induced by boundary migration, might involve additional dissipation of energy, in other words, a triple junction might have a finite mobility. A theoretical consideration of triple junction motion was reported in [47]. It is stressed that the steady-state motion of such a system can only be correctly measured for a very limited set of geometrical configurations. One of them is shown in Fig. 17. This problem of joint grain boundary—triple junction motion was solved in a quasi two-dimensional approximation, assuming a uniform GB model (i.e., both the surface tension σ and the mobility m_b are the same for all grain boundaries and independent of boundary orientation) [47]—and some very important features of the kinetics of the motion of such systems were derived. In particular, it was shown that the steady-state motion of the system as a whole is indeed possible.

The behavior of the system can be discussed in terms of the parameter Λ which describes the drag influence of the triple junction on the migration of the GB system

$$\Lambda = \frac{m_j a}{m_b} = \frac{2\theta}{2\cos\theta - 1} \tag{12}$$

where m_j is the mobility of the triple junction, 2θ is the vertex angle and a the width of the consumed grain (Fig. 17).

For large values of ($\Lambda \gg 1$) the junction does not drag the migration, and the angle θ tends to attain the equilibrium value $\pi/3$. In this case the velocity V of the system movement as a whole is independent of the mobility of the triple junction and is determined by the boundary mobilities and the driving force (corresponding to the width of the grain) [47]:

$$V = \frac{2\pi m_b \sigma}{3a} \tag{13}$$

When $\Lambda \ll 1$, the steady state velocity V is controlled by the mobility of the junction:

$$V = \sigma m_j \tag{14}$$

In this case the angle θ tends to zero.

The shape of the GB system in the steady-state motion was predicted for both uniform GB model and the case when the system is symmetric relative to the x-axis, i.e., the grain boundaries 1 and 2 are the same, but different from boundary 3: $\sigma_1 = \sigma_2 = \sigma \neq \sigma_3$;

$$m_{b_1} = m_{b_2} = m_b \neq m_{b_3}.$$

For the latter situation the velocity of triple junction can be expressed as

$$V = m_j(2\sigma\cos\theta - \sigma_3) \tag{15}$$

and the steady-state value of the angle θ is

$$\frac{2\theta\sigma}{2\sigma\cos\theta - \sigma_3} = \frac{m_j a}{m_b} = \Lambda. \tag{16}$$

The criterion parameter Λ defines the drag influence of the triple junction on the migration[1].

In Fig. 18 the shape of a moving GB system with triple junction at different temperatures is shown. The system comprises two $61^\circ\langle 11\bar{2}0\rangle$ high-angle curved grain boundaries and a straight 3° tilt GB (not visible on the micrograph, it extends from the tip of the junction parallel to the straight legs of the high-angle grain boundaries). The solid line on the second and fifth frame represents the theoretical shape of the tricrystal with reasonable agreement between experiment and calculation. A strong temperature dependence of the angle θ can be noticed, which cannot be attributed to the temperature dependence of the surface tension [26] (Fig. 19), rather the observed change of the angle θ has to be associated with the kinetics of the system.

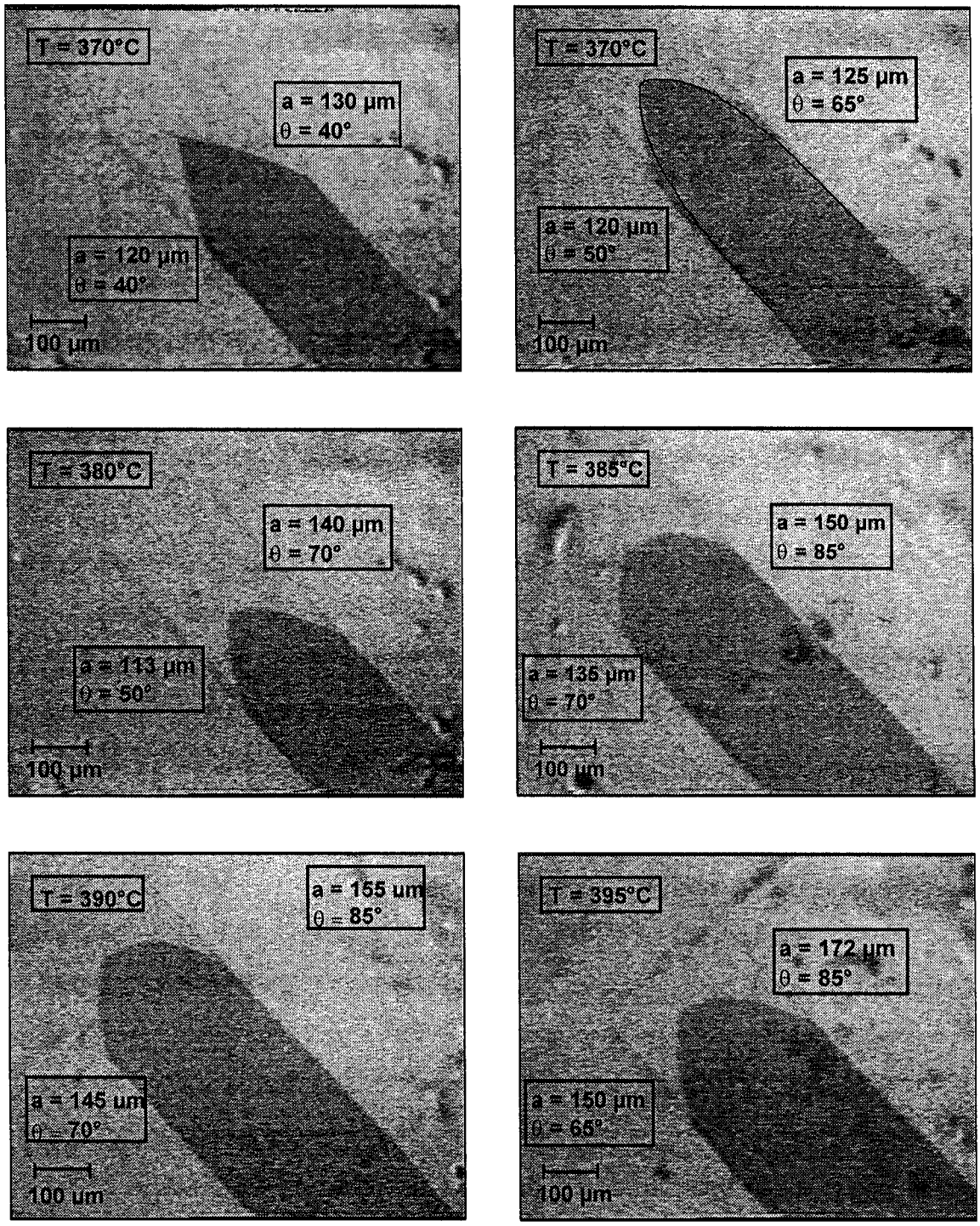

Figure 18. Shape of a moving grain boundary half-loop with triple junction. The solid line on the second picture represents the theoretical shape. (Zn tricrystal, misorientation angles of the tilt grain boundaries about $\langle 11\bar{2}0 \rangle$ are 61°, 61°, and 3°.)

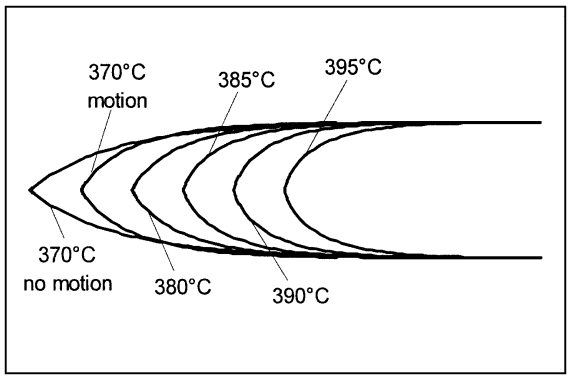

Figure 19. Vertex configuration at the triple junction at different temperatures (Zn tricrystal, misorientation angles of the tilt grain boundaries about $\langle 11\bar{2}0\rangle$ are 61°, 61°, and 3°).

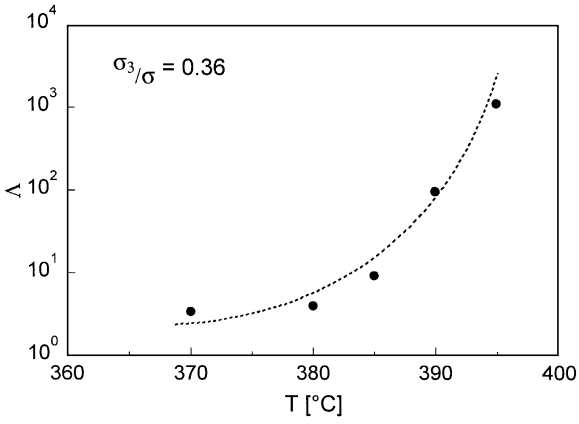

Figure 20. Temperature dependence of the parameter Λ for the investigated Zn tricrystal.

The value of the criterion parameter Λ, which defines, by which kinetics—GB or triple junction—the motion of the system is controlled, can be estimated on the basis of the given approach. As can be seen at relatively "low" temperatures, the motion of the system is governed by the mobility of the triple junction, whereas at "high" temperatures the motion is controlled by the mobility of the high-angle GB. Also, the transition from triple junction to boundary kinetics was observed [26] (Fig. 20). Similar results were obtained on GB systems with another set of grain boundaries [27].

The current observations demonstrate for the first time, that triple junctions can act as pinning centers and in certain cases are able to control the kinetics of GB systems. There is some indirect evidence of this already in polycrystal behavior, e.g., the time dependence of the mean grain size in the early stages of grain

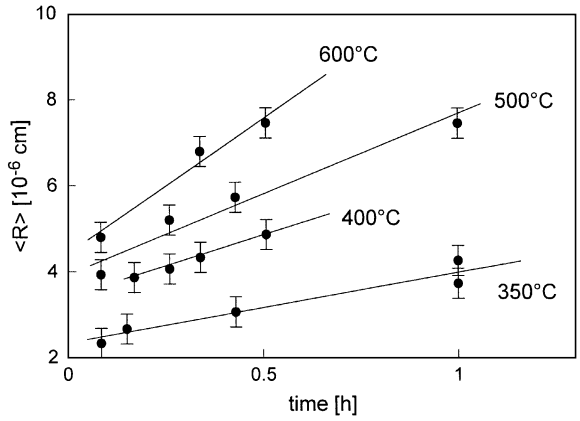

Figure 21. Time dependence of the mean grain size in thin silver films at different temperatures [48].

growth. The point is that during motion of a GB system controlled by GB mobility the velocity V is proportional to the curvature ($\sim 1/a$, Eq. (13)), while for the motion governed by the triple junction mobility the velocity V is unrelated to geometry (Eq. (14)). As a consequence, the mean grain size during grain growth will change in proportion to the square root time if GB mobility dominates ($\langle D\rangle \sim \sqrt{t}$), while the mean grain size has to be proportional to the annealing time if the triple junction mobility controls ($\langle D\rangle \sim t$). Such experimental data were indeed obtained in a study of grain growth in thin (∼1000 Å) silver films [48]. The time dependencies of the mean grain size early in the grain growth at different temperatures are represented in Fig. 21. The linear dependence between the mean grain size and the time of annealing is obvious, and what is of importance, the linear law of grain growth is replaced by a parabolic one at a later stage of the process.

Acknowledgment

The authors are grateful for financial support by the Deutsche Forschungsgemeinschaft and to the Russian Foundation for Fundamental Research under contract N96-02-17483 for financial support of their cooperation.

Note

1. One can see that the ratio m_b/m_j has a dimension of a length. Since the grain boundary mobility and the mobility of the triple junction are thermally activated quantities, it is unlikely that this ratio is in the range of an interatomic distance.

References

1. K.T. Aust and J.W. Rutter, Trans. AIME **215**, 119 (1959).
2. K.T. Aust and J.W. Rutter, Trans. AIME **215**, 820 (1959).
3. K.T. Aust and J.W. Rutter, Acta Metall. **13**, 181 (1965).
4. R.C. Sun and C.L. Bauer, Acta Metall. **18**, 635 (1970).
5. R. Viswanathan and C.L. Bauer, Acta Metall. **21**, 1099 (1973).
6. M.S. Masteller and C.L. Bauer, Scripta Metall. **10**, 1033 (1976).
7. E.M. Fridman, Ch.V. Kopetskii, L.S. Shvindlerman, and V.Yu. Aristov, Z. Metallk. **64**, 458 (1973).
8. E.M. Fridman, Ch.V. Kopetskii, and L.S. Shvindlerman, Z. Metallk. **66**, 533 (1975).
9. V.Yu. Aristov, V.L. Mirochnik, and L.S. Shvindlerman, Sov. Phys. Solid State **18**, 137 (1976).
10. V.G. Sursaeva, A.V. Andreeva, Ch.V. Kopetskii, and L.S. Shvindlerman, Phys. Met. Metall. **41**, 98 (1976).
11. V.Yu. Aristov, V.E. Fradkov, and L.S. Shvindlerman, Phys. Met. Metall. **45**, 83 (1978).
12. G. Gottstein and L.S. Shvindlerman, Scripta Metall. Mater. **27**, 1521 (1992).
13. K. Lücke and K. Detert, Acta Metall. **5**, 628 (1957).
14. J.W. Cahn, Acta Metall. **10**, 789 (1962).
15. K. Lücke and H.P. Stüwe, in *Recovery and Recrystallization of Metals*, edited by L. Himmel (Interscience, New York, 1963), p. 171.
16. C.S. Smith, Trans. Am. Inst. Min. Engrs. **175**, 15 (1948).
17. G. Gottstein and L.S. Shvindlerman, Acta Metall. Mater. **41**, 3267 (1993).
18. V.Yu. Aristov, V.E. Fradkov, and L.S. Shvindlerman, Sov. Phys. Solid State **22** 1055 (1980).
19. J. Verhasselt, G. Gottstein, D.A. Molodov, and L.S. Shvindlerman (to be published).
20. Ch.V. Kopetskii, L.A. Musikhin, and L.S. Shvindlerman, Sov. Phys. Solid State **13**, 620 (1971).
21. A.V. Antonov, Ch.V. Kopetskii, L.S. Shvindlerman, and V.G. Sursaeva, Sov. Phys. Dokl. **18**, 736 (1974).
22. P.F. Schmidt, Doctoral thesis, Universität Münster (1975).
23. J. Gastaldi and C. Jourdan, Phys. Stat. Sol. (a) **49**, 529 (1978).
24. V.Yu. Aristov, Ch.V. Kopetskii, D.A. Molodov, and L.S. Shvindlerman, Sov. Phys. Solid State **22**, 1900 (1980).
25. U. Czubayko, D. Molodov, B.-C. Petersen, G. Gottstein, and L.S. Shvindlerman, Measurement Science and Technology **6**, 947 (1995).
26. L.S. Shvindlerman, G. Gottstein, U. Czubayko, and V.G. Sursaeva, in *Proc. of Rex'96, the Third Intern., Conf. on Recrystallization and Related Phenomena*, edited by T.R. McNelly (MIAS, Monterey, 1997), p. 255.
27. V.G. Sursaeva, U. Czubayko, G. Gottstein, and L.S. Shvindlerman (to be published).
28. V.Yu. Aristov, Ch.V. Kopetskii, and L.S. Shvindlerman, in *Theoretical Fundamentals of Materials Science* (Moscow, Nauka, 1981), p. 84.
29. G. Ibe, W. Dietz, A.C. Fraker, and K. Lücke, Z. Metallk. **61**, 498 (1970).
30. G. Ibe and K. Lücke, in *Recrystallization, Grain Growth and Textures*, edited by H. Margolin (American Society of Metals, Metals Park, Ohio, 1966), p. 434.
31. D.A. Molodov, U. Czubayko, G. Gottstein, and L.S. Shvindlerman, Scripta Metall. Mater. **32**, 529 (1995).
32. G. Gottstein, D.A. Molodov, U. Czubayko, and L.S. Shvindlerman, J. de Phys. **C3**(5), 89 (1995).
33. G. Gottstein, H.C. Murmann, G. Renner, C. Simpson, and K. Lücke, in *Textures of Materials*, edited by G. Gottstein and K. Lücke (Springer Verlag, Berlin, 1978), p. 521.
34. D. Udler and D.N. Seidman, Interface Sci. **3**, 41 (1995).
35. D.A. Molodov, U. Czubayko, G. Gottstein, L.S. Shvindlerman, B. Straumal, and W. Gust, Phil. Mag. Lett. **72**, 361 (1995).
36. K. Lücke, Canadian Metallurgical Quarterly **13**, 261 (1974).
37. F. Haessner and S. Hofmann, in *Recrystallization of Metallic Materials*, edited by F. Haessner (Dr. Riederer Verlag GmbH, Stuttgart, 1978), p. 63.
38. S.E. Babcock and R.W. Balluffi, Acta Metall. **37**, 2357 and 2367 (1989).
39. S. Hashimoto and B. Baudelet, Scripta Metall. **23**, 1855 (1989).
40. N.F. Mott, Proc. Phys. Soc. **60**, 391 (1948).
41. R.J. Jhan and P.D. Bristowe, Scripta Metall. **24**, 1313 (1990).
42. B. Schönfelder, D. Wolf, S.R. Phillpot, and M. Furtkamp, accepted for publication in Interface Science.
43. S. Ahoron and A. Brokman, Acta Metall. Mater. **39**, 2389 (1991).
44. D.A. Molodov, J. Swiderski, G. Gottstein, W. Lojkowski, and L.S. Shvindlerman, Acta Metall. Mater. **42**, 3397 (1994).
45. E.L. Maksimova, B.B. Straumal, V.E. Fradkov, and L.S. Shvindlerman, Phys. Met. Metall. **56**, 133 (1983).
46. G. Gottstein and L.S. Shvindlerman (to be published).
47. A.V. Galina, V.E. Fradkov, and L.S. Shvindlerman, Phys. Met. Metall. **63**, 165 (1987).
48. V.G. Sursaeva, Mater. Sci. Forum **62–64**, 807 (1990).